
CONFORMATIONAL REGULATION IN SINGLE MOLECULE REACTIONS

L.N. CHRISTOPHOV^{1,2}, A.R. HOLZWARTH³, V.N. KHARKYANEN²

UDC 539.199

© 2003

¹Bogolyubov Institute for Theoretical Physics, Nat. Acad. Sci. of Ukraine
(Kyiv, Ukraine),

²Institute of Physics, Nat. Acad. Sci. of Ukraine
(Kyiv, Ukraine),

³Max-Planck-Institut für Strahlenchemie
(Mülheim a.d. Ruhr, Germany)

Modern methods of single-molecule detection and spectroscopy make it possible to directly monitor the long series of reaction cycles of one macromolecule in real time. Within the previously developed theory of substrate-conformation interaction, we give a simple method of calculating the main statistical characteristics of single-molecule trajectories reflecting the modulation of a reaction cycle by the slow conformational dynamics of the macromolecule. Computer simulations show considerable qualitative distinctions of such characteristics from those calculated within the standard chemical/Michaelis kinetics.

Introduction

In viewing the role of structural motions of a macromolecule (enzyme) in the reaction it performs, two aspects can be conventionally distinguished. The first concerns the influence of a structural relaxation on the reaction course within a single reaction act (single turnover of the protein). This has been studied in detail on the model system of rebinding CO to myoglobin, see e.g. [1]; the corresponding theory proposed in the milestone paper [2] still remains rather workable. The second is related to slower, regulatory conformational re-arrangements that could be essential in a sequence of multiple turnovers and are able to drastically change the functional cycle of the enzyme. This has been discussed mostly in the biochemical literature in the context of “kinetic cooperativity” exhibited by some monomeric enzymes [3, 4]. Such enzymes were called “hysteretic” [3]. The implication involved was that there exist the slow (as compared to the reaction rates) conformational transitions of the enzyme and thereby its memory about the preceding reaction act. Models of true hysteretic (from physical point of view) behaviour of macromolecules, implying bistability and emergence

of their new working states due to intramolecular non-equilibrium phase transitions controlled by the substrate flux, were proposed in our theory of molecular self-organization ([5, 6] and refs. therein). With the advent of single-molecule spectroscopy (see e.g. reviews [7, 8]), it becomes possible to directly prove that the effects of dynamical disorder [9] and structural memory can be really crucial for the enzyme mode of operation. The properties of stochastic trajectories of hundreds of successive turnovers of a single enzyme (see e.g. [10, 11]) clearly show a non-Markovian character of the stationary reaction course. These experiments, especially those on the enzymatic cycle of cholesterol oxidase [11], initiated a series of theoretical papers [12–16] on modelling single molecule reactions within the schemes with both discrete and continuous sets of conformational sub-states.

Evaluation of the models was based on their ability to reproduce the statistical characteristics of single molecule trajectories. These characteristics are, in the first place, the on-time distributions (OTD) and auto-correlation functions (ACF) of some marker (e.g. fluorescent cofactor [11]) labelling the state of reagents in a supposedly Michaelis-Menten scheme¹. In simple two- or three-state schemes of conventional chemical kinetics, the OTD and ACF have typical forms containing 1–2 decaying time exponentials. Experiments [10, 11] clearly demonstrate that it is not the case. It is the description of the details of this non-exponentiality originated from conformational mobility that was the main aim of works [12–16].

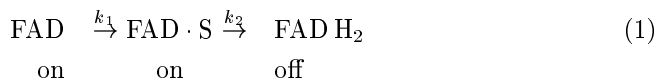
In the present work, we emphasize incompleteness and shortcomings of previous models for the calculation of the mentioned statistical characteristics. These drawbacks are rooted just in ignoring the flow conditions (multiple turnovers of the macromolecule) and the

¹More complex correlation characteristics are also subject to intensive study (e.g. [12, 13, 15, 16])

feedback between the reagent states and conformational subsystem. We show that this could lead to an inadequate interpretation of the reaction mechanism. To avoid this, within the previously developed theory of substrate-conformation interaction, we propose a simple and consistent algorithm of calculation of the OTD and ACF. Their specific new features, reflecting a non-trivial conformational regulation, can be seen even in the two-state model, as is shown with illustrative computer simulations.

1. Models of the Influence of Conformational Mobility upon the Reaction. Calculation of OTD and ACF

Oxidation of cholesterol and its derivatives, studied at the single molecule level in [11], is a very convenient model system. The enzyme cholesterol oxidase possesses a cofactor (FAD) that is fluorescent in the non-reduced state and non-fluorescent in the reduced state. Under certain conditions, the reaction can be analyzed within the three-state scheme



or even the two-state scheme



that present the limiting steps of the full two-stage Michaelis scheme of the oxidation of the substrate S by oxygen [11, 12]. Notations “on”/“off” indicate the presence/absence of fluorescence. In both cases (1) and (2), experiment results in a record of successive on-off fluorescence flips like a telegraph signal. In view of serial turnovers, there is of course a reverse process to the initial FAD state to meet a new substrate², so that schemes (1), (2) imply at least one back reaction. Here the key point is whether we can consider the initial state of the next turnover identical to that of the previous turnover *or* conformational changes of the enzyme (cofactor) have no time to relax to a negligible extent.

If the protein structure is sufficiently rigid, then the kinetics in schemes (1), (2) are trivial. Consequently, analyzing on-time histograms and OTD/ACF shapes yields nothing new as compared to conventional chemical kinetics applicable to

²Sometimes the “substrate” can be one and the same, as e.g. an electron in a “charge separation — recombination” closed loop [5, 6], or a ligand rebinding to its site after photo-dissociation (the Mb-CO model [17]).

bulk/ensemble experiments. Recall that in this case the OTD in the two-state scheme $\mathbf{1} \xrightleftharpoons[k_{-1}]{k_1} \mathbf{0}$ (state $\mathbf{1}$ is supposed to be fluorescent) is determined by the decay equation

$$\frac{dp_1(t)}{dt} = -k_1 p_1(t), \quad (3)$$

where $p_1(t)$ is the probability to find the system in state $\mathbf{1}$ (or the population of this state in the bulk case). Denoting the OTD as $f_{\text{on}}(t)$, one has a Poisson distribution of the residence time t of the system in state $\mathbf{1}$ if at $t = 0$ the system has jumped to this state, $p_1(0) = 1$:

$$\begin{aligned} f_{\text{on}}(t) &= -\frac{dp_1(t)}{dt} = \frac{dp_0(t)}{dt} = k_1 e^{-k_1 t}; \\ \langle t \rangle &= \int_0^{\infty} t f_{\text{on}}(t) dt = \frac{1}{k_1}. \end{aligned} \quad (4)$$

As for the off-time distribution, its expression differs from Eqs.(3),(4) in replacing k_1 by k_{-1} and the initial condition $p_1(0) = 1$ by $p_0(0) = 1$ only. The ACF of fluorescence is also one-exponential with the rate constant $(k_1 + k_{-1})$ that is typical of a standard dichotomous noise with the mean transition rates k_1 and k_{-1} (see e.g. [12]). In the three-state scheme with allowance for the enzyme-substrate complex, $\mathbf{1} \xrightarrow{k_1} \mathbf{2} \xrightarrow{k_2} \mathbf{0} \xrightarrow{k_3} \mathbf{1}$, both states $\mathbf{1}$ and $\mathbf{2}$ are fluorescent, but the fluorescence decay is determined by the sink from state $\mathbf{2}$ only (input to state $\mathbf{0}$) provided that $p_1(0) = 1$:

$$\begin{aligned} f_{\text{on}}(t) &= \frac{dp_0(t)}{dt} = k_2 p_2(t); \\ p_1(0) &= 1, \quad p_2(0) = p_0(0) = 0. \end{aligned} \quad (5)$$

Then it is easy to obtain:

$$\begin{aligned} f_{\text{on}}(t) &= \begin{cases} \frac{k_1 k_2}{k_1 - k_2} (e^{-k_2 t} - e^{-k_1 t}), & k_1 \neq k_2; \\ k_1 t e^{-k_1 t}, & k_1 = k_2; \end{cases} \\ \langle t \rangle &= \frac{k_1 + k_2}{k_1 k_2}. \end{aligned} \quad (6)$$

Allowing for k_{-1} makes the expressions slightly bulkier but preserves the two-exponent character of $f_{\text{on}}(t)$: the rise determined by the larger of rate constants and the decay determined by the smaller (Fig.1). Basing on qualitative distinctions of the curve shapes in Fig.1, they

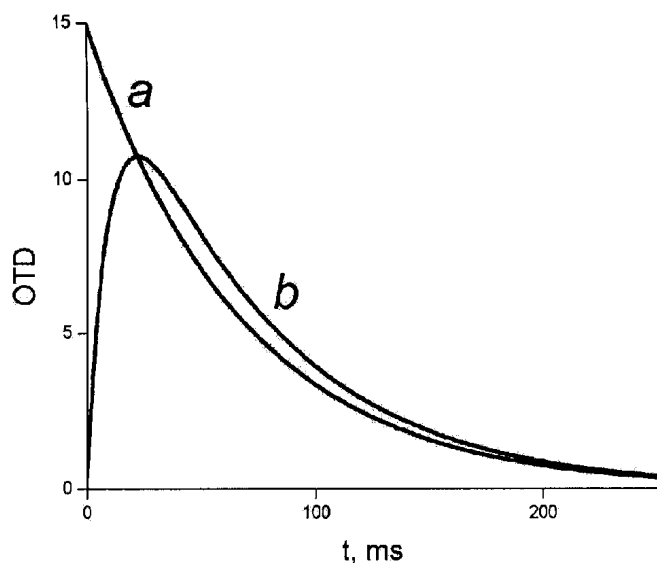


Fig.1. *a* – OTD (4) for scheme (2), $k_1 = 15 \text{ s}^{-1}$; *b* – OTD (6) for scheme (1), $k_2 = 15 \text{ s}^{-1}$, $k_1 = 100 \text{ s}^{-1}$

usually conclude on the necessity to take into account the intermediate states of the substrate-enzyme complex, the role of the substrate binding stage, etc. [11, 18]. Below we will see that even such an obvious conclusion may turn out to be wrong under noticeable substrate-conformation interaction coupling. In particular, non-monotonic OTD like shown in Fig.1, *b* may appear even in a two-state scheme.

Let us turn to the methods of taking into account the protein structure motions, that is, to the consideration of conformational sub-states of a relevant two-state or three-state scheme. The simplest (and most frequently applied to explaining the deviations from simple exponential kinetics) way is to complicate the scheme by duplicating the number of sub-states differing in reaction rates. This is the two-conformation, or 2×2 , model; the 2×3 or $2 \times N$ (that is, with 3 or N sub-states) models have been also considered [13, 16, 19]. In regard the models that are discrete in conformational sub-states, it is worth noting the following.

Duplicating (triplating, so on) the number of these states adds one (two, so on) exponential to the OTD/ACF time dependences whereas the latter obtained in experiments are, as a rule, essentially non-exponential³. Besides, postulating, say, the presence of two conformations means implicitly the existence of two minima of the structural potential both in the “ground”

³Note also that such kinetic models are linear by definition and do not admit the self-organization effects due to a nonlinear feedback between the substrate flux and the structure subsystem (see the discussion in [5]).

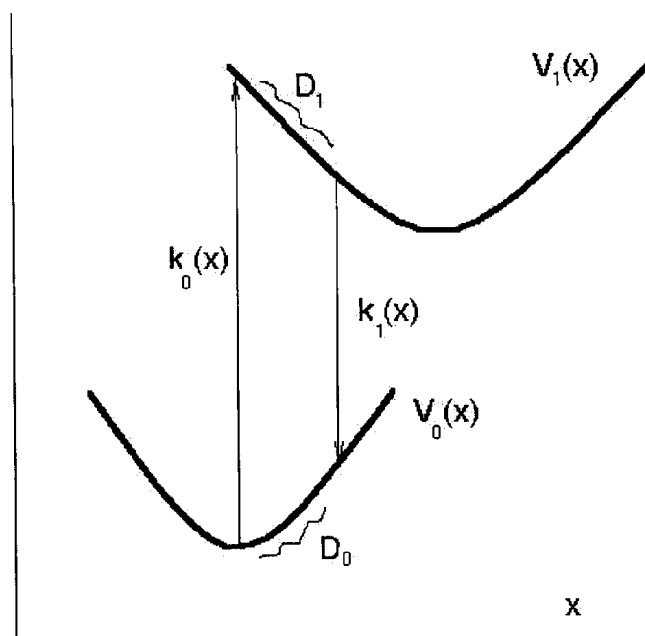


Fig.2. The scheme of processes in a reversible reaction (two-state model with conformational diffusion)

and “excited” states of proteins (that is, in the states corresponding to an attached and detached ligand, substrate, etc.). Although this potential possesses a hierarchical structure [1], its roughness can be often ignored under physiological temperatures [20]; then it is more natural to suppose that, depending on the substrate presence, the conformational sub-system tends to one minimum — of course, different in different states of the substrate-enzyme system. In each of these potentials, there proceeds its own diffusion process along the *continuous* variable x , accompanied by the decay with generally x -dependent rates (see Fig.2). Although the scheme in Fig.2 represents two Agmon–Hopfield processes (or “half-reactions” [13]), combining them into a closed loop adds a new quality. It is quite obvious that now the next turnover can noticeably differ from the preceding one since the probability distribution in potential $V_0(x)$ might have no time to be reset. The primary role in this memory effect belongs to the diffusion coefficient D_0 in the “lower” state (though all the other structural parameters of the system — steepnesses of the potentials, their relative positions, etc. — are also important). In real systems, the rate constant $k_0(x)$ reflects a kind of “pumping” (e.g., light intensity in a system of photochemical charge separation in a donor-

acceptor pair of an isolated photosynthetic reaction center, or substrate concentration in an enzymatic reaction) and can be often thought as non-distributed [6, 12, 14, 21]. It is clear that, under weak pumping and sufficiently fast diffusion in $V_0(x)$, no memory effect could be seen as the thermally equilibrium distribution in $V_0(x)$ will be re-established before every turnover. However, under increasing pumping and/or decreasing D_0 , the structural memory can strongly affect the reaction course, especially if the dependence $k_1(x)$ is sufficiently pronounced. In many cases, the latter could be reasonably thought as $\sim \exp(-x)$ [5, 6, 12, 14, 21] rather than $\sim x^2$ supposed in the “bottleneck” problems [22]. Under certain relations between system’s parameters, a new stable stationary state of the macromolecule coupled with the substrate flux can emerge⁴ in a threshold way with respect to flux intensity. Two possible cycles with slow and fast reaction rates (i.e., values of x close to positions of minima of V_1 and V_0) can co-exist in a certain bistability domain [5, 21]. Previously, we showed the evidences for protein structure memory in ensemble experiments [6]. Needless to say, they should be directly seen in single molecule experiments just in the simplest statistical characteristics like the OTD and ACF.

The reaction scheme depicted in Fig.2 was extended to the three-state case by Agmon [14] to fit the experimental data of [11] and to elucidate the character of protein motion along the “perpendicular coordinate” x in the course of a single “conformational cycle”. Correspondingly, the structure memory effects, as will be clear slightly below, remained beyond his consideration.

Proceed now to the analysis of the OTD and ACF in the model shown in Fig.2. The given process can be thought as the action of a dichotomous noise with its mean transition rates $k_0(x)$, $k_1(x)$ upon the structural coordinate x . The corresponding jumps result in the instantaneous exchange of structural potentials $V_0 \rightarrow V_1$ and diffusion coefficients $D_0 \rightarrow D_1$ and vice versa⁵. The noise itself, however, is x -dependent. Thus, there exists the *feedback* between the discrete variable $n \in \{0,1\}$ and continuous variable x . This crucial point is sometimes ignored in treatments of the modulation of the reaction by slow conformational motions: a corresponding Fokker–Planck or Smoluchowski equation does not contain any sink terms [12] or is identical for both **1** and **0** states [15].

⁴Such a possibility was pointed out by Neet, see e.g. [3], p.194.

⁵As usual, structural motions are supposed to be overdamped.

The model in Fig.2 can be cast to the following equations [5]:

$$\begin{aligned} \frac{\partial p_0(x,t)}{\partial t} &= D_0 \frac{\partial}{\partial x} \left(\frac{dV_0}{dx} + \frac{\partial}{\partial x} \right) p_0(x,t) - \\ &- k_0(x)p_0(x,t) + k_1(x)p_1(x,t), \\ \frac{\partial p_1(x,t)}{\partial t} &= D_1 \frac{\partial}{\partial x} \left(\frac{dV_1}{dx} + \frac{\partial}{\partial x} \right) p_1(x,t) + \\ &+ k_0(x)p_0(x,t) - k_1(x)p_1(x,t) \end{aligned} \quad (7)$$

(here and below, V_i ’s are supposed dimensionless, i.e. expressed in $k_B T$ -units. Also dimensionless is x , as we do not specify its nature that could be geometric, energetical, etc., see [5, 6, 17, 21] for details).

Mapping Eq.(7) to the experiments [11, 18] and scheme (2), set state **1** fluorescent (non-reduced cofactor). Then state **0** corresponds to the reduced non-fluorescent cofactor. In [11, 18], the two-state system was supposed to be adequate for the reaction of oxidation of cholesterol derivatives at high substrate concentrations (assuming k_1 rate-limiting).

1. O T D. The OTD is now given by an obvious generalization of Eq.(4):

$$f_{\text{on}}(t) = \int k_1(x)p_1(x,t)dx, \quad (8)$$

where, however, $p_1(x,t)$ is the solution not to set (7) but to the sink-Smoluchowski (Agmon–Hopfield) equation

$$\frac{\partial p_1(x,t)}{\partial t} = D_1 \frac{\partial}{\partial x} \left(\frac{dV_1}{dx} + \frac{\partial}{\partial x} \right) p_1(x,t) - k_1(x)p_1(x,t) \quad (9)$$

provided that the initial distribution, according to the very sense of the on-time notion, is normalized to unity:

$$\int p_1(x,0)dx = 1. \quad (10)$$

Eq.(10) is, however, an integral initial condition only and does not specify the initial conformation distribution that is necessary for solving Eq.(9) and then computing $f_{\text{on}}(t)$ (8). We should suppose further that the stochastic flips of fluorescence reflect (in a sufficiently long series of turnovers) the reaction course as a stationary random process. Then it is reasonable to assume that the distribution in conformations at the instant of a flip to state **1** (“on”) corresponds to the steady-state distribution in x in state **0** (“off”), i.e. just before the flip. Of course, this steady-state distribution is determined

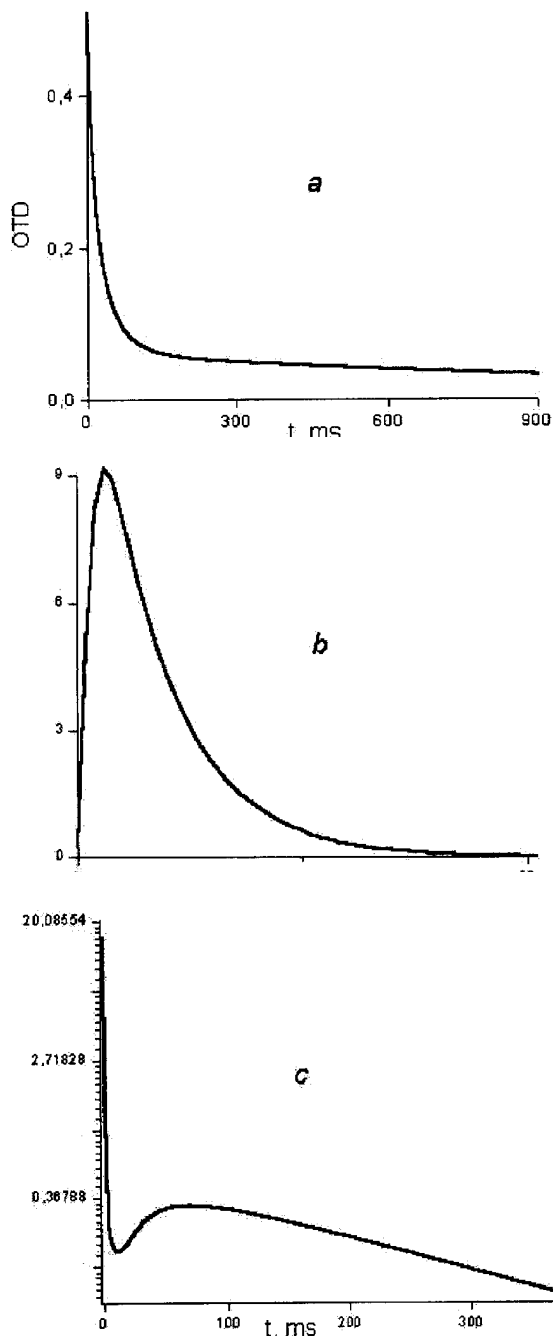


Fig.3. OTD in the two-state model. $k_1(x) = k_1^0 e^{-x}$, k_0 non-distributed. *a*, *b* — harmonic potentials $V_n = \gamma_n(x - x_n)^2$. *a* — $x_0 = 3, x_1 = 5, k_0 = 0.01, k_1^0 = 0.1, \gamma_0 = \gamma_1 = 10, D_0 = 0.1, D_1 = 0.001$; *b* — $x_0 = 7, x_1 = 2, k_0 = 0.1, k_1^0 = 1, \gamma_0 = \gamma_1 = 10, D_0 = D_1 = 0.1$; *c* — anharmonic potentials (11), $x_0 = 5, x_1 = 3, k_0 = 0.1, k_1^0 = 1, \gamma_0 = \gamma_1 = 25, \alpha_i = 0, \lambda_i = 1, D_0 = 0.1, D_1 = 0.01$

⁶This procedure could be of course described in terms of propagators, as was done e.g. in [13] for a discrete scheme, see also [19]. In many cases, however (in particular, the case of exponential sink under present consideration), it is difficult to find the Green function explicitly and then the latter loses its advantages for practical calculations.

by both equations of set (7). Therefore, we arrive at the following algorithm for calculating OTD⁶:

1) solve set (7) (with arbitrary initial conditions) to find the steady-state distribution $p_{0,1}(x, t = \infty) \equiv p_{0,1}^{st}(x)$;

2) normalize the solution $p_0^{st}(x)$ to *unity* (since, by the OTD definition, one has to consider the decay of fully populated state **1**), $F(x) = p_0^{st}(x) / \int dx p_0^{st}(x)$;

3) take the function $F(x)$ as the initial condition to Eq.(9): $p_1(x, 0) = F(x)$. From (9), find $p_1(x, t)$ and calculate OTD (8).

We now underline the main point of such a method of calculating the OTD. In contrast to the statement made in [13] that “the measurements of on-time and off-time clearly separate the forward and backward half-reactions”, we see that, in fact, this is not so. With allowance for slow conformational mobility, the on-time and off-time are not completely independent any longer, as both these quantities are determined by all the system parameters and not only by those of on- or off-state. Thus, the OTD is determined by not only $k_1(x)$ and even not only $k_1(x)$ and $k_0(x)$ but also by drift and diffusion parameters in *both* states and by relative positions of potentials $V_0(x)$ and $V_1(x)$ as well: it is the quantities that determine the initial conditions to Eq.(9). We can thereby expect the possible effects of inter-cycle influence, i.e. memory effects, exhibiting themselves even in the simplest statistical characteristics of stochastic single molecule trajectories, prior to calculating correlations of the fourth order and higher or correlations of on-time events separated by several cycles (that might require too precise/long trajectories, so far unavailable).

Of course, supposing $p_0^{st}(x)$ to be thermally equilibrium, $p_0^{st}(x) \sim \exp(-V_0(x)/k_B T)$, as was taken in [14], we will not reveal any memory effects. However, the steady-state solutions to set (7) are not obliged to be thermally equilibrium at all. On the contrary, they imply essentially non-equilibrium conditions, with permanent input of substrates, light energy, so on, determined by “pumping” k_0 .

Fig.3 shows three examples of the calculated $f_{on}(t)$ in the two-state model with $k_1(x) = k_1^0 e^{-x}$ and k_0 non-distributed [2, 5, 6, 12]. While the OTD in Fig.3,*a* remains monotonic (although far from being Poisson-like), the OTD in Fig.3,*b* is rather similar to a typical one in a *three-state* scheme despite the absence of any third state of the enzyme-substrate complex. Curves in

Figs.3,*a* and 3,*b* are calculated with harmonic potentials $V_n(x)$. In [6, 23], we employed more realistic potentials of limited growth,

$$V_n(x) = \frac{\gamma_n}{2}(x - x_n)^{2(1+\alpha_n)} \frac{\lambda_n}{\lambda_n^2 + (x - x_n)^2} \quad (11)$$

($\alpha_n \ll 1$), harmonic within Lorentzian half-width λ_n (all parameters are dimensionless). Fig.3,*c* exemplifies the OTD in the a two-state scheme with potentials (11). It reminds the “echo” effect described in [13] for a more sophisticated differential correlation between separated on-time events; here it is obtained just for the OTD.

The results in Fig.3 mirror the course of structure relaxation that could be qualitatively explained with schemes like shown in Fig.2 for given mutual positions of the potentials and corresponding stationary distributions $p_0(x)$'s. As follows from (8), the OTD is nothing but evolution of the mean rate constant of state **1** decay. For example, in the case of Fig.3,*a*, where the initial distribution (not shown) is concentrated near $x_0 \sim 3$ to the left of the minimum of $V_1(x)$, its greater part decays very fast ($k_1^{-1}(x_0) \sim 10\text{ms}$) due to comparatively large value $D_0 = 0.1$. The smaller part of $p_0(x)$ (getting shifted to larger x due to D_1) decays hundred times slower. While inverting the mutual position of the potentials ($V_1(x)$ to the left of $V_0(x)$) drastically changes the very OTD shape, reducing it to the pseudo-three-state case (Fig.3,*b*). Now the initial distribution, concentrated near $x_0 = 7$, should first get shifted to the left to gain the decay rate and, therefore, the most part of it decays with some delay (that is mirrored with a one-maximum curve). Due to comparatively fast diffusion in $V_1(x)$, here the time scale is much shorter than that in Fig.3,*a*. Finally, at the parameter values in Fig.3,*c* the initial distribution is bimodal. Then, after the very fast decay of the left peak of $p_0(x)$, some delay in the decay of the right peak occurs (like in the case *b*); this entails an “unusual” shape of the curve.

We can see that even the two-state continuous scheme with simple one-well potentials shows, apart from the non-exponentiality, rather non-trivial manifestations of structural regulation even in the simplest single molecule characteristics, OTD. The same is true for the simplest correlation function of the second order, ACF (see below).

2. A C F. Autocorrelation of fluorescence in single-molecule experiments like described in [11] implies the correlations of the yes-no random variable ξ with its space of states $\{0,1\}$ corresponding to the absence or the presence of fluorescence, respectively. The normalized

ACF of fluorescence fluctuations is defined as

$$C_2(t) \equiv C(t) = \frac{\langle \Delta\xi(t)\Delta\xi(0) \rangle}{\langle \Delta\xi^2 \rangle} = \frac{\langle \xi(t)\xi(0) \rangle - \langle \xi \rangle^2}{\langle \xi^2 \rangle - \langle \xi \rangle^2}, \quad (12)$$

where $\Delta\xi = \xi - \langle \xi \rangle$. For the dichotomous random variable $\xi \in \{\xi_1, \xi_0\}$ with $\xi_1 = 1$, $\xi_0 = 0$, one has $\langle \xi \rangle = \langle \xi^2 \rangle = \dots = \langle \xi^n \rangle$, so that $\langle \Delta\xi^2 \rangle = \langle \xi \rangle(1 - \langle \xi \rangle)$.

By definition,

$$\langle \xi(t)\xi(0) \rangle = \sum_{i,j} \xi_i \xi_j P(\xi_i, t; \xi_j, 0), \quad i = 0, 1, \quad (13)$$

where $P(\xi_i, t; \xi_j, 0)$ is the joint probability to find $\xi = \xi_i$ at instant t and $\xi = \xi_j$ at instant 0. The only non-vanishing term of sum (13) corresponds to $i = j = 1$, so that

$$\langle \xi(t)\xi(0) \rangle = P(1, t; 1, 0) = P(1, t | 1, 0)P^{\text{st}}(1), \quad (14)$$

where $P^{\text{st}}(1)$ is the stationary probability of fluorescence (recall that we suppose the random process to be stationary with time-independent averages) and simply reads

$$P^{\text{st}}(1) = \langle \xi \rangle = \int dx p_1^{\text{st}}(x), \quad (15)$$

as state **1** is fluorescent. As regards $P(1, t | 1, 0)$, it is the conditional (transition) probability

$$P(1, t | 1, 0) = \int dx p_1(x, t) \quad (16)$$

to observe fluorescence at instant t provided that it was observed at instant 0. As in the case with OTD, here we need to correctly define the initial conditions to Eq.(7). Now we should start also from the fully populated fluorescent state **1**. However, the initial distribution in conformations, as distinct from the OTD case, corresponds to the steady-state distribution just in the same state **1**. Besides, to calculate then $p_1(x, t)$, we should now use both the equations of set (7). Finally, the algorithm is as follows:

- 1) solve set (7), now to find the steady-state distribution $p_1(x, t = \infty) \equiv p_1^{\text{st}}(x)$;
- 2) normalize it (and not p_0^{st} as we need to calculate the probability $\mathbf{1} \rightarrow \mathbf{1}$) to unity: $\Phi(x) = p_1^{\text{st}}(x) / \int dx p_1^{\text{st}}(x)$;
- 3) again solve set (7), now with initial conditions $p_1(x, 0) = \Phi(x)$, $p_0(x, 0) = 0$

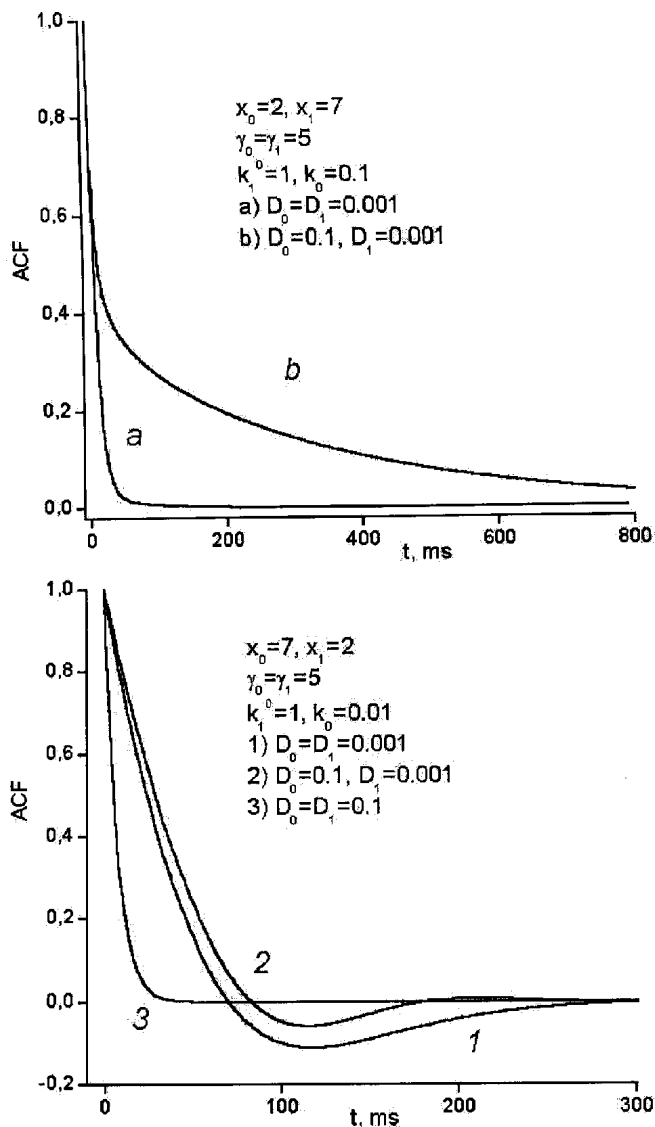


Fig.4. ACF in the two-state model. Harmonic potentials $V_n = \gamma_n(x - x_n)^2$; $k_1(x) = k_1^0 e^{-x}$, k_0 non-distributed

4) and calculate $P(1, t | 1, 0)$ (16) with $p_1(x, t)$ found. Then, with allowance for Eqs.(12)–(15), obtain ACF (17):

$$C(t) = \frac{P(1, t | 1, 0) - \langle \xi \rangle}{1 - \langle \xi \rangle}. \quad (17)$$

Depending on the relative positions of potentials V_i 's, various ACF behaviours (up to oscillating) are possible, see Fig.4. As in Section 1, it could be explained (and easily seen in computer simulations performed) by the course of structure relaxation. Note that it follows from (16), (17) that $C(t)$ reproduces, in fact, the evolution of the integral population of state 1

(from its “overpopulated” to steady-state value at a given “pumping”). For example, curve *a* of the upper plot, corresponding to the initial distribution $p_1(x)$ concentrated near $x \sim 7$ (not shown in Fig.4), mirrors the fast decay of a very small excess portion $\sim 1\%$ in the left tail of the distribution; then the system remains mostly in fluorescent state 1 as $\langle \xi \rangle \sim 0.99$ at the given values of parameters. Increasing D_0 to 0.1 (curve *b*) makes the initial distribution bimodal with a noticeable peak at $x \sim 2$. Yet after the fast disappearing of this part, the evolution is not completed since the final distribution $p_1(x, t = \infty)$ should become bimodal again. This occurs due to the “probability spilling over” from the domain $x \sim 7$ of the main pumping (D_0 is large) to the domain $x \sim 2$. This slower process is mirrored in the second phase of the ACF.

Under the potential position inversion and certain parameter values, the steady state establishment could be of oscillating character. Thus, curve 2 of the lower plot in Fig.4 corresponds to the evolution for the domain of x between 3 and 7. The initial decay of the left part is very fast and too excessive. Then the repeated populating of the upper state from the domain near $x \sim 7$ follows, again somewhat excessive, and finally some necessary leakage from this domain to the left comes after ~ 200 ms. Obviously, such an “unusual behaviour” of both the OTD and especially oscillating ACF could be revealed under explicit allowing for turnover multiplicity only.

3. Three-state scheme. Proceed to the reaction scheme with an intermediate state, $1 \xrightarrow{k_1} 2 \xrightarrow{k_2} 0 \xrightarrow{k_0} 1$. It can be mapped to the set [14]

$$\begin{aligned} \frac{\partial p_1(x, t)}{\partial t} &= D_1 \frac{\partial}{\partial x} \left(\frac{dV_1}{dx} + \frac{\partial}{\partial x} \right) p_1(x, t) - \\ &- k_1(x)p_1(x, t) + k_0(x)p_0(x, t), \\ \frac{\partial p_2(x, t)}{\partial t} &= D_2 \frac{\partial}{\partial x} \left(\frac{dV_2}{dx} + \frac{\partial}{\partial x} \right) p_2(x, t) + \\ &+ k_1(x)p_1(x, t) - k_2(x)p_2(x, t), \\ \frac{\partial p_0(x, t)}{\partial t} &= D_0 \frac{\partial}{\partial x} \left(\frac{dV_0}{dx} + \frac{\partial}{\partial x} \right) p_0(x, t) + \\ &+ k_2(x)p_2(x, t) - k_0(x)p_0(x, t). \end{aligned} \quad (18)$$

Following (1) and [11], here two states (1 and 2, both correspond to $\xi = 1$) are fluorescent (corresponding to non-reduced FAD in the reaction of cholesterol oxidation [11]). In this case, our considerations above should be properly modified, but the main idea remains valid. Therefore, we restrict ourselves with expounding the calculation algorithm.

OTD. Find steady-state solutions $p_i^{\text{st}}(x)$, $i = 0, 1, 2$, to set (18). Normalize $p_0^{\text{st}}(x)$ to unity and then take it for $p_1(x, 0)$ (together with $p_2(x, 0) = 0$) as initial conditions to set (19):

$$\begin{aligned} \frac{\partial p_1(x, t)}{\partial t} &= D_1 \frac{\partial}{\partial x} \left(\frac{dV_1}{dx} + \frac{\partial}{\partial x} \right) p_1(x, t) - \\ &- k_1(x) p_1(x, t), \\ \frac{\partial p_2(x, t)}{\partial t} &= D_2 \frac{\partial}{\partial x} \left(\frac{dV_2}{dx} + \frac{\partial}{\partial x} \right) p_2(x, t) + \\ &+ k_1(x) p_1(x, t) - k_2(x) p_2(x, t) \end{aligned} \quad (19)$$

that is, to set (18) at $k_0 = 0$. Then calculate the OTD with the use of Eq.(19) analogously to (8):

$$f_{\text{on}}(t) = \int k_2(x) p_2(x, t) dx. \quad (20)$$

ACF. With the steady-state solutions $p_i^{\text{st}}(x)$'s of set (18), construct the following initial conditions:

$$p_1(x, 0) = \frac{p_1^{\text{st}}(x)}{\langle \xi \rangle}; \quad p_2(x, 0) = \frac{p_2^{\text{st}}(x)}{\langle \xi \rangle}; \quad p_0(x, 0) = 0, \quad (21)$$

where

$$\langle \xi \rangle = \int dx [p_1^{\text{st}}(x) + p_2^{\text{st}}(x)] \quad (22)$$

is the steady-state probability of fluorescence. Then solve set (18) with initial conditions (21) and calculate the function

$$P(1, t | 1, 0) = \int dx [p_1(x, t) + p_2(x, t)]. \quad (23)$$

Inserting Eqs.(22),(23) into Eq.(17) yields the ACF. Of course, one can expect not a less variety of the ACF behaviour than in the two-state scheme.

Fitting the OTD and ACF to the experimental data on oxidation of cholesterol derivatives [11] gives essentially the same parameter values as obtained by Agmon [14]. This coincidence, however, has turned out to be incidental since we found out that, in this specific case, the OTD and ACF are quite insensitive to the value of D_0 (the parameter of "memory" ignored by Agmon); thus, its value given in [14] makes not too much sense. At the same time, should the distance $|x_1 - x_0|$ between the minima of V_1 and V_0 be greater by one unit only, our algorithm would reveal an essential dependence of the OTD on D_0 whereas Agmon's method would not, by definition.

Final Remarks

The strategic goal of this paper was to pave the way to unveiling the underlying mechanism of conformational regulation as probed in single-molecule experiments. We tried to stress the significance of explicit allowance for non-equilibrium flux conditions and the feedback between the reaction states and conformational motions. Both these elements enter the initial equations (7), (18) of our theory explicitly. This, as well as the algorithms proposed to calculate the OTD and ACF, seems to be a new step in the studies in the field.

The indicative examples given above of "unusual" (as compared to previously reported [10–14, 18]) behaviour of the OTD and ACF show the strong influence of these elements upon the latter. Precisely, under flow conditions (indispensable in all experiments of the kind), the OTD becomes dependent on all parameters of the substrate-conformation system and not only on the parameters of a "half-reaction" [13] connected with the on-state. Even in the two-state case, the OTD may acquire the shape considered preciously as inherent in the three-state reaction only (cf. Fig.1,b to Fig.3,b or results in [10, 11, 14]). The types of the OTD like that in Fig.3,c or the oscillating ACF like shown in Fig.4, bottom, are reported for the first time. A comparison of the fittings in our approach and in that ignoring the structure memory of a macromolecule [14] also is in favor of the theory proposed here.

We deliberately omit calculations of correlation characteristics of higher orders. Although this could be done, it would most likely imply the requirement of very long and precise trajectories. Besides, should they be available, a more interesting effect could be traced, showing the role of structure memory perhaps better than the obvious non-Markovity of turnovers. We mean the clear change of a cycle from that in the initial part of a sufficiently long trajectory to its final part, or even the co-existence of two types of cycles in the bistability domain. This would be an excellent proof of accumulation of slow structural changes and the corresponding non-linear phenomena of the emergence of new functional states of a working enzyme [3, 5, 6].

We thank N.M. Berezetskaya for programming. L.Ch. gratefully acknowledges support from the DAAD and Kyiv SRC "Vidhuk".

1. Frauenfelder H., Wolynes P.G., Austin R.H.// Rev. Mod. Phys. — 1999. — **71**. — P.S419–S430.
2. Agmon N., Hopfield J.J.// J. Chem. Phys. — 1983. —**78**.— P.6947–6959.

3. Neet K.E., Ainslie G.R.// Meth. Enzymol. — 1980. —**64**.— P.192—227.
4. Cornish-Bowden A., Luz Cardenas M.// J. Theor. Biol. — 1987.—**124**. — P.1—27.
5. Christophorov L.N., Holzwarth A.R., Kharkyanen V.N., van Mourik F.// Chem. Phys. — 2000.—**256**.— P.45—60.
6. Barabash Yu.M., Berezetskaya N.M., Christophorov L.N. et al.// J. Chem. Phys. — 2002.—**116**.— P.4339—4352.
7. Xie X.S., Trautman J.K.// Ann. Rev. Phys. Chem. — 1998.—**49**.— P.441—480.
8. Weiss S.// Science. — 1999.—**283**.— P.1676—1683.
9. Zwanzig R.// Acc. Chem. Res. — 1990.—**23**.— P.148—152.
10. Edman L., Rigler R.// PNAS USA. — 2000.—**97**. — P.8266—8271.
11. Lu H.P., Xun L., Xie X.S.// Science. — 1998.—**282**.— P.1877—1882.
12. Schenter G.K., Lu H.P., Xie X.S.// J. Phys. Chem. A. — 1999.—**103**.— P.10477—10488.
13. Cao J.// Chem. Phys. Lett. — 2000.—**327**.— P.38—44.
14. Agmon N.// J. Phys. Chem. B. — 2000.—**104**.— P.7830—7834.
15. Yang S., Cao J.// Ibid. — 2001.—**105**.— P.6536—6549.
16. Yang H., Xie X.S.// Chem. Phys. — 2002.—**284**.— P.423—437.
17. Nienhaus G.U., Mourant J.R., Chu K., Frauenfelder H.// Biochemistry. — 1994.—**33**.— P.13413—13430.
18. Xie X.S., Lu H.P.// J. Biol. Chem. — 1999.—**274**.— P.15967—15970.
19. Bargesov V., Chernyak V., Mukamel S.// J. Chem. Phys. — 2002.—**116**.— P.4240—4251.
20. Zwanzig R.// PNAS USA. — 1988.—**85**.— P.2029—2030.
21. Goushcha A.O., Kharkyanen V.N., Scott G.W., Holzwarth A.R.// Biophys. J. — 2000.—**79**.— P.1237—1252.
22. Zwanzig R.// J. Chem. Phys. — 1992.—**97**.— P.3587—3589.

23. Goushcha A.O., Manzo A.J., Scott G.W. et al.// Biophys. J. — 2003.—**84**.— P.1146—1160.

КОНФОРМАЦІЙНА РЕГУЛЯЦІЯ РЕАКЦІЙ ПОДИНОКИХ МАКРОМОЛЕКУЛ

Л.М. Христофоров, А.Р. Хольцварт, В.М. Харкянен

Резюме

Сучасні методи детектування та спектроскопії поодиноких молекул дозволяють безпосередньо спостерігати довгі серії реакційних обертів однієї й тієї ж макромолекули у реальному часі. У межах розвинутої нами раніше теорії субстрат-конформаційної взаємодії ми подаємо простий спосіб обчислення головних статистичних характеристик одномолекулярних траєкторій, що несуть інформацію про модуляцію реакційного циклу повільними конформаційними рухами макромолекули. Комп'ютерні симуляції показують значні якісні відмінності цих характеристик від таких, що розраховані у межах стандартної (біо)хімічної кінетики.

КОНФОРМАЦИОННАЯ РЕГУЛЯЦИЯ РЕАКЦИЙ ОДИНОЧНЫХ МАКРОМОЛЕКУЛ

Л.М. Христофоров, А.Р. Хольцварт, В.М. Харкянен

Резюме

Современные методы детектирования и спектроскопии одиночных молекул позволяют прямые наблюдения длинных серий реакционных оборотов одной и той же макромолекулы в реальном времени. В рамках развитой нами ранее теории субстрат-конформационных взаимодействий предлагается простой способ вычисления основных статистических характеристик одномолекулярных траекторий, несущих информацию о модуляции реакционного цикла медленными конформационными движениями макромолекулы. Компьютерные симуляции показывают значительные качественные отличия этих характеристик от полученных в рамках стандартной (био)химической кинетики.